Available online at www.sciencedirect.com
SCIENCE DIRECT
Chemical Physics Letters 419 (2006) 458–463
CHEMICAL PHYSICS LETTERS
www.elsevier.com/locate/cplett

# Enhanced field emission from $O_2$ and $CF_4$ plasma-treated CuO nanowires

Y.W. Zhu [a,b], A.M. Moo [b], T. Yu [a], X.J. Xu [b,c], X.Y. Gao [a], Y.J. Liu [a], C.T. Lim [b,c], Z.X. Shen [a], C.K. Ong [a], A.T.S. Wee [a,b], J.T.L. Thong [b,d], C.H. Sow [a,b,*]

[a] *Department of Physics, National University of Singapore (NUS), Block S12, 2 Science Drive 3, Singapore 117542, Singapore*
[b] *National University of Singapore Nanoscience and Nanotechnology Initiative, Singapore*
[c] *Department of Mechanical Engineering and Division of Bioengineering, NUS, 9 Engineering Drive 1, Singapore 117576, Singapore*
[d] *Department of Electrical and Computer Engineering, NUS, 4 Engineering Drive 3, Singapore 117576, Singapore*

Received 19 October 2005; in final form 22 November 2005
Available online 27 December 2005

**Abstract**

The effects of tetrafluoro methane ($CF_4$) and oxygen ($O_2$) plasmas on the morphology and field emission of copper oxide (CuO) nanowires are investigated. The tip diameter of nanowires is found to be reduced and the tips sharpened by both plasmas. Furthermore, $O_2$ plasma removes the amorphous layer on the surface of as-grown nanowires, while $CF_4$ plasma treatment deposits a thick amorphous coating which results in a decrease in the surface work function. All these factors contribute to the large enhancement of the field emission performance after the plasma treatment.
© 2005 Elsevier B.V. All rights reserved.

## 1. Introduction

Cold cathodes or electron field emitters attract much attention because of their advantages over conventional thermionic emitters, such as low energy consumption [1]. Among the many published works, a great deal of effort has been devoted to carbon-based nanomaterials, especially carbon nanotubes (CNTs), due to their high aspect ratio and high chemical stabilities [2]. Besides CNTs, a wide variety of one-dimensional (1D) nanostructures, such as nanowires have been of great interest to researchers. Large and stable field emission (FE) currents from the nanowires have been reported [3–6]. Recently, experiments have shown that plasma treatments can functionalize carbon-based materials and improve their FE performance, and the effects of plasmas from $H_2$ [7], Ar [8], $O_2$ [9], $CF_4$ [10] and $NH_3$ [11] gases have been investigated. Comparatively, fewer detailed studies on the plasma treatment of inorganic nanowires have been reported [12].

Among different nanowires considered for field emitters, CuO nanowires have been successfully synthesized using a simple method by various groups [13–15]. With excellent FE properties [16,17], CuO nanowires are good candidates for investigating the effects of plasma treatments on nanowires. Thus, similar to our previous efforts on CNTs [18], $O_2$ and $CF_4$ plasmas from a reactive ion etching (RIE) system were used to further treat as-grown CuO nanowires in this work. The changes in their morphologies, surface structures and components were monitored and the enhanced FE properties investigated.

## 2. Experimental setup and procedures

The vertically aligned CuO nanowire films were prepared by directly heating Cu plates on a hotplate under ambient conditions, as described in our previous work [13]. The growth temperature was about 350 °C and growth time was about 2 days. For plasma treatment, as-grown samples were placed inside the chamber of a SAMCO RIE-10N Reactive Ion Etching Unit. Samples were exposed to the plasma produced from $O_2$ (35 sccm)

* Corresponding author. Fax: +65 6777 6126.
*E-mail address:* physowch@nus.edu.sg (C.H. Sow).

0009-2614/$ - see front matter © 2005 Elsevier B.V. All rights reserved.
doi:10.1016/j.cplett.2005.11.087

or $CF_4$ (15 sccm) gas, respectively. Typically, the exposure lasted for 5 or 10 min. Other details of the RIE process can be found in another report [18].

With the assistance of focused laser pruning method [19], some channels were created on the CuO nanowire films. Some nanowires near a channel were then identified for comparison of the tip dimensions of these individual nanowires before and after plasma treatments. The as-grown and treated samples were characterized by scanning electron microscopy (SEM, JEOL JSM-6400F), transmission electron microscopy (TEM, JEOL JEM-2010F; operating at 200 kV), X-ray Photoelectron Spectroscopy (XPS, ESCA MK II; Mg source), micro Raman spectroscopy (Jobin Yvon T64000) and ultraviolet photoelectron spectroscopy (UPS, Surface, Nanostructure and Interface Science (SINS) beamline at Singapore Synchrotron Light Source (SSLS)). The measurements of FE properties of as-grown and plasma-treated nanowires were carried out using a two-parallel-plate configuration in a vacuum chamber with a pressure of about $5 \times 10^{-7}$ Torr. The distance between electrodes was kept at 150 μm.

## 3. Results and discussion

A channel was made by laser pruning on the as-grown CuO nanowire films and some nanowires nearby the edge were chosen for the analysis as shown in Fig. 1a. Fig. 1b,c show the same region of CuO nanowires before and after 10 min of $O_2$ RIE treatment by focusing on the part of Fig. 1a marked by a dotted box. From this region, a nanowire (marked by a circle) was further magnified as shown in the insets of Fig. 1b,c, respectively. After 10 min of $O_2$ plasma treatment, the average diameter near its tip was reduced from about 159 to 144 nm, i.e., a reduction of almost 10%. In addition, some nanowires became bent and slightly shortened, e.g., the nanowire indicated by the arrow in Fig. 1c. In a similar way, the effects of $CF_4$ plasma on a given nanowire were investigated as shown in Fig. 1d,e and their insets. The average diameter of the selected nanowire was reduced from about 91 to 81 nm and was shortened by about 30 nm after the exposure of $CF_4$ plasma for 10 min. By comparing additional 10 individual nanowires after plasma etching, it was deduced that the tip diameter was reduced by an average value of 9 nm after both $O_2$ and $CF_4$ plasma treatments.

Fig. 2 shows the TEM and HRTEM images of CuO nanowires before and after plasma treatments. Although the as-grown nanowires with sharp tips were observed, more than half of them had a flat tip as shown in Fig. 2a. Also, almost all as-grown nanowires were covered by an amorphous layer with an average thickness of several nanometers, as is typically demonstrated by the inset of Fig. 2a. Such layer was still characterized to be CuO and could be induced during cooling after growth. In contrast, after 10 min of $O_2$ (Fig. 2b) and $CF_4$ (Fig. 2c) plasma etching, all observed nanowires had sharp tips and no flat tips were found. Moreover, the surface of the tip region was found to be cleaner after $O_2$ plasma treatment, and the

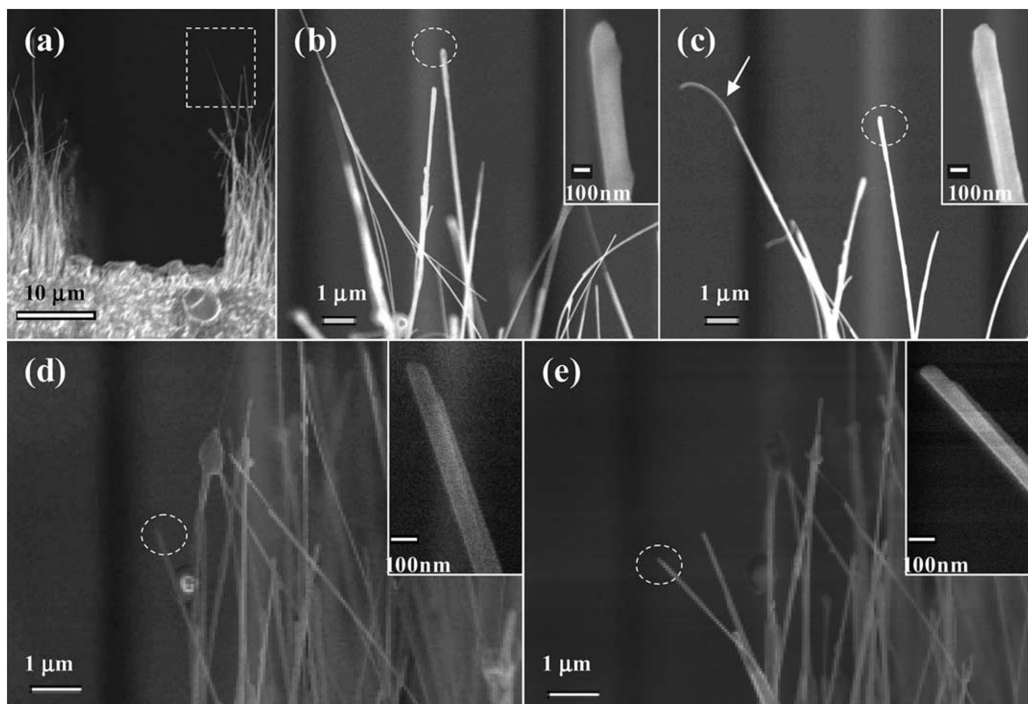


Fig. 1. (a) SEM image showing side view of a channel pruned by laser on CuO nanowire films. The dotted box shows the region of interest magnified in (b) as made and (c) after 10 min of exposure to $O_2$ RIE. The insets of (b) and (c) show high magnification SEM images of the same nanowire (in the white circle) before and after RIE, respectively. (d) a region and a nanowire (inset) before $CF_4$ RIE; (e) the same region and nanowire (inset) after exposure to 10 min of $CF_4$ RIE.

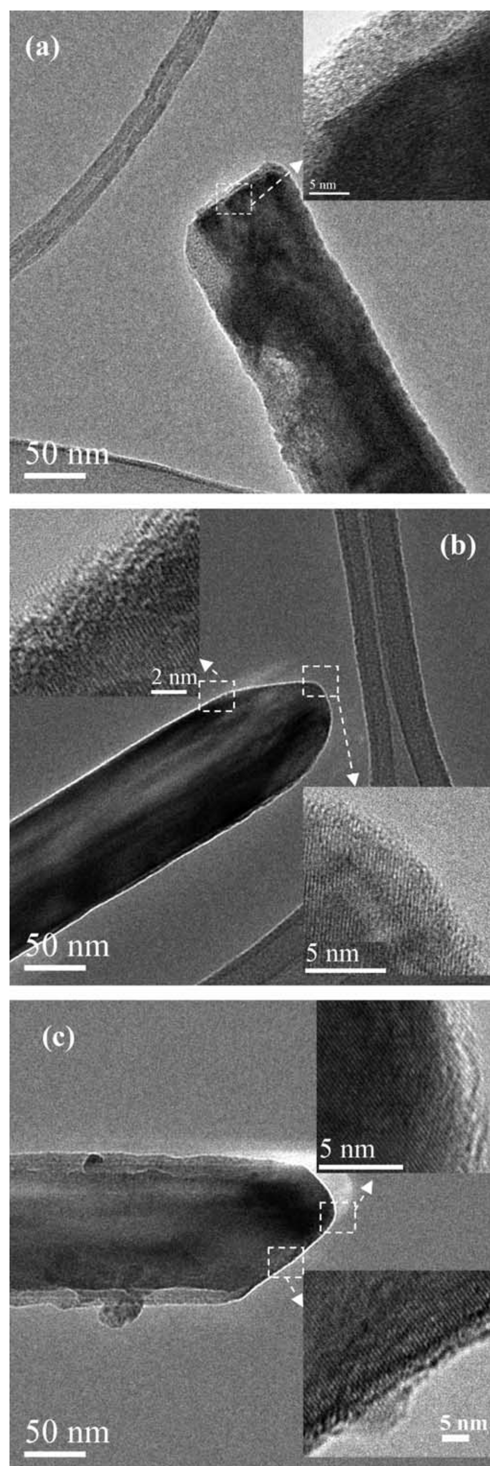


Fig. 2. (a) TEM image of an as-grown CuO nanowire. The inset shows a HRTEM image from the tip part. (b) TEM image of a CuO nanowire after exposure to 10 min of $O_2$ RIE. Insets are the HRTEM images of different parts. (c) TEM image of a CuO nanowire after 10 min of $CF_4$ RIE.

amorphous layers disappeared. From the insets of Fig. 2b, the crystalline structures are clearly seen to have extended up to the surface. On the other hand, $CF_4$ plasma treatment formed another amorphous layer coating onto the surface as shown in Fig. 2c and its insets. The top right inset of Fig. 2c demonstrates clear crystalline structures, but the bottom right inset shows an amorphous layer with a thickness of 1–2 nm. On the cylindrical body of the nanowire, this amorphous layer becomes much thicker, even more than that of as-grown CuO nanowires.

To investigate the chemical nature of the amorphous layer on the surface of CuO nanowires after 10 min of $CF_4$ RIE treatment, XPS study was carried out. The XPS spectra of F 1s and Cu 2p peaks are shown in Fig. 3a,b, respectively. From Fig. 3a, we can see that after $CF_4$ plasma treatment, a strong two-peak F 1s spectrum appears. By deconvoluting with Gaussian peaks after subtraction of background, four sub-peaks are further observed. Those peaks at 684.7 and 685.7 eV can be ascribed to the F–Cu bonding in $CuF_2$ and the other two at 689.1 and 690.2 eV are possibly due to the presence of $(–CF_2–CF_2–)n$ bonds [20]. The occurrence of fluorinated carbon and copper could be reasonably attributed to the 10 min of $CF_4$ plasma treatment. Moreover, after $CF_4$ plasma treatment (Fig. 3b), the Cu 2p peaks tend to shift to higher binding energy due to the formation of strong

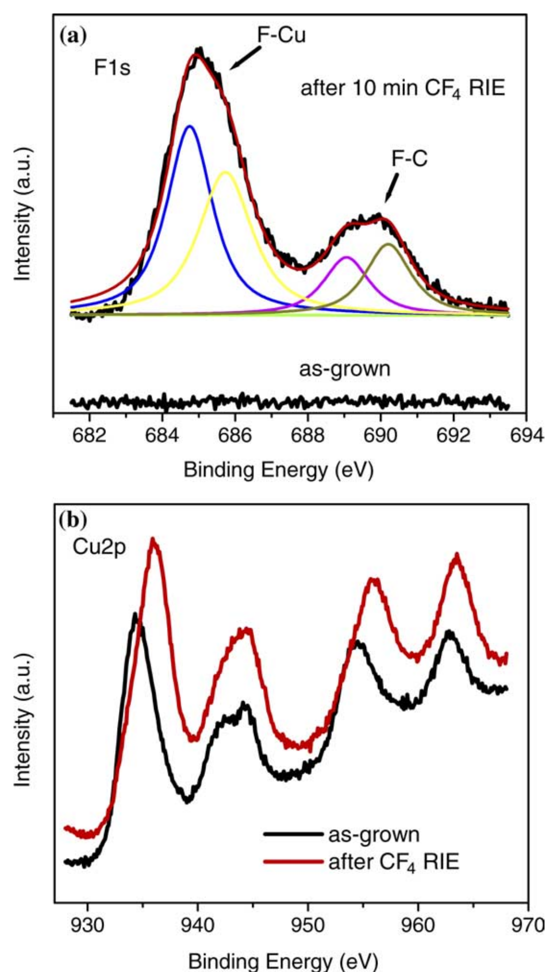


Fig. 3. XPS spectra of (a) F 1s and (b) Cu 2p for as-grown and $CF_4$ plasma-treated CuO nanowires.

Cu–F bonds, since the binding energy of Cu 2p in $CuF_2$ is larger than that in CuO [20].

Micro Raman spectra are shown in Fig. 4a. Three peaks are observed from the as-grown CuO nanowires, corresponding to the $A_g$, $B_g^{(1)}$ and $B_g^{(2)}$ modes due to the vibrations of oxygen atoms in the CuO structures [21,22]. After $O_2$ plasma treatment, the positions and widths of all peaks remained unchanged; but $CF_4$ plasma treatment slightly shifts the spectra to higher wave numbers and an asymmetrical $A_g$ peak is observed. Such a shift and asymmetrical peak could be due to the introduction of surface amorphous layer during plasma treatments [23].

UPS was carried out under ultrahigh vacuum ($10^{-11}$ Torr) to study the effects of plasma treatment on the work function of CuO nanowire films. Fig. 4b shows the inelastic cutoff and the Fermi edges of the as-grown, $O_2$ and $CF_4$ plasma-treated samples. The photon energy was 49.7 eV, and −20 V bias was applied to the samples so that the sample inelastic cutoff could be distinguished from that due to the spectrometer. The work function can be obtained from $\phi = h\nu - \Delta E$ [24], where $h\nu$ is the photon energy (49.7 eV) and $\Delta E$ is the spectrum width, the distance between the sample inelastic cutoff and Fermi edges. Thus, from Fig. 4b and its inset, it can be seen that 10 min of $O_2$ plasma etching only slightly changes the work function of CuO nanowires; but 10 min of $CF_4$ RIE reduces it by about 0.5 eV. In addition, the absolute work function values are estimated to be about 4.5, 4.5 and 4.0 eV for as-grown, $O_2$ and $CF_4$ plasma-treated CuO nanowires, respectively. All the values are lower than that of bulk CuO [25]. It is worth noting that these values are quite close to that from the field emission of aligned CuO nanofibrils [26], but obviously higher than our previous results [17] and other reports [16]. This difference could be due to the lower vacuum in the FE chamber (order of $10^{-7}$ Torr) than that in UPS measurements, the high sensitivity of FE results to the detailed sample morphologies and the simplified morphological assumption in the estimation of [17].

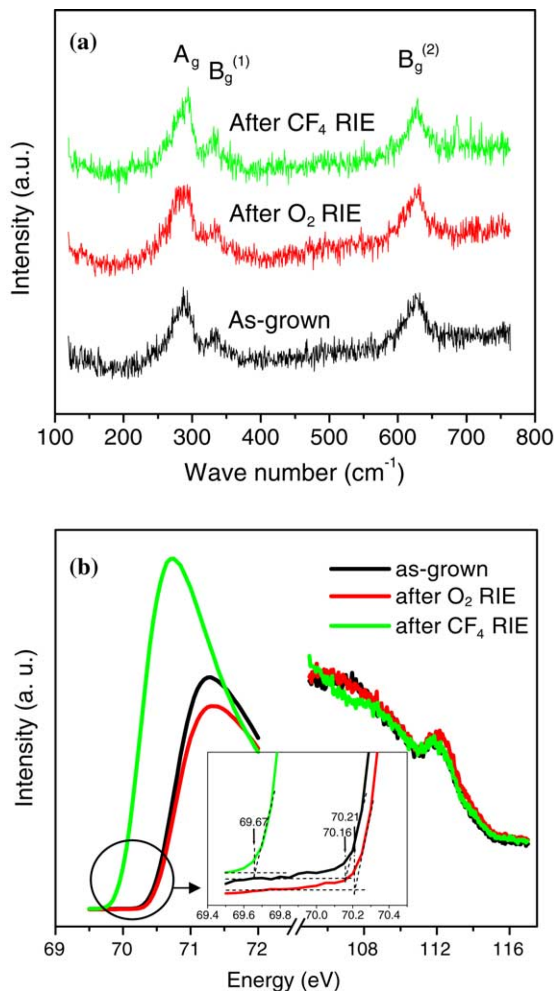


Fig. 4. (a) Micro Raman spectra of as-grown and plasma-treated CuO nanowire films. (b) The inelastic cutoff and Fermi edges of CuO nanowires before and after treatments. The inset shows magnified inelastic cutoff edge.

Finally, the FE properties of plasma-treated CuO nanowires were measured. Fig. 5a shows the results from the same sample before RIE, after 5 and 10 min of exposure to $O_2$ plasma. We can see that after 5 min of etching, the maximal current density (under the field of 5.3 V/μm) increases from the original 0.13 to 0.34 mA/cm$^2$ and another 5 min RIE further enhances it to 0.54 mA/cm$^2$. At the same time, the turn-on field (corresponding to the current density of 10 μA/cm$^2$) decreases from 3.6 V/μm to 3.2 and 3.0 V/μm after 5 and 10 min of exposure to $O_2$ plasma, respectively. In the same way, the field emission of another sample was improved by $CF_4$ RIE (Fig. 5b). The maximal current density is enhanced by 25 times from 0.04 to 1 mA/cm$^2$ after 10 min of exposure to $CF_4$ plasma. The turn-on field was reduced from 4.2 to 3.7 V/μm.

To explore the possible mechanisms, the Fowler–Nordheim (FN) equation [27] was used to analyze the FE data:

$$J(E) = \frac{\alpha A}{\phi}(E_l)^2 \exp\left(-\frac{B\phi^{3/2}}{E_l}\right), \tag{1}$$

where $J$ (A/cm$^2$) is the macroscopic current density, $E$ (V/μm) is the average electric field, $E_l$ (V/μm) is the local field near the emitters, $\phi$ (eV) is the work function, $A$ and $B$ are constants and $\alpha$ is an area factor, which is equal to the ratio of an actual emitting surface area to an overall surface area, describing the geometrical efficiency of electron-field emission [28]. By defining an enhancement factor $\beta = E_l/E$, from Eq. (1), $\alpha$ and $\beta$ can be expressed by the slope ($S$) and ordinate intercept ($i$) of FN plots ($\ln(J/E^2)$ versus $1/E$):

$$\beta = -\frac{B\phi^{3/2}}{S} \tag{2}$$

and

$$\alpha = \frac{S^2 e^i}{AB^2\phi^2}. \tag{3}$$

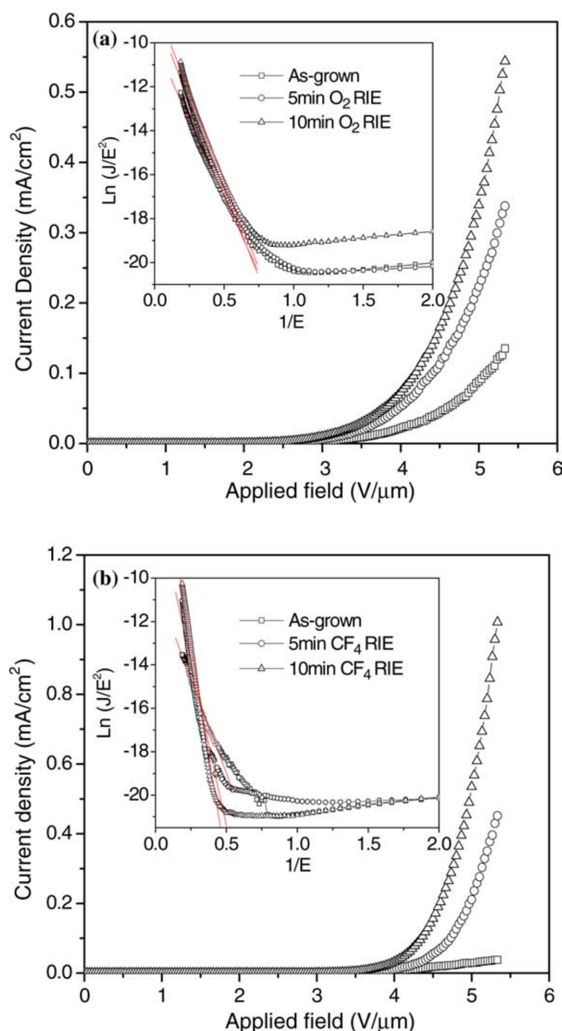


Fig. 5. (a) Typical field emission *J–E* curves and FN plots (inset) of as-grown and $O_2$ plasma-treated CuO nanowires. (b) Typical field emission *J–E* curves and FN plots (inset) of as-grown and $CF_4$ plasma-treated CuO nanowires.

By fitting the FN plots, the slopes and intercepts are obtained. Here, we add a subscript 0 to represent the results from as-grown samples and 1 to represent those after 10 min of plasma treatments. Thus, for both $O_2$ and $CF_4$ RIE, the following relationships result from Eqs. (2) and (3): $\frac{\beta_1}{\beta_0} \leqslant 1$ and $\frac{\alpha_1}{\alpha_0} \ll 1$, which suggest that after plasma treatments, the enhanced FE may not be caused by the increased average enhancement factors, but may be related to larger effective emission areas [29]. Actually, many nanowires become bent after plasma treatments, which may increase the effective FE emission area due to exposure of the side walls [17], as has been previously suggested for rough surfaces [30].

Another possible explanation for the enhanced FE after $O_2$ plasma treatment is the cleaner surface structures. Previous results have demonstrated that strong electron scattering can occur at the interface between the amorphous surface layer and crystalline core, which may encumber the FE properties of as-grown CuO nanowires [31]. $O_2$ plasma can also generate copper superoxides ($CuO_x$, $x = 2$, 3, 4) which can improve the conductivity of indium–tin oxide (ITO) [32]. Such improvements can also play a role on the CuO nanowires after $O_2$ plasma treatment and, thus enhance their FE performance. Furthermore, plasma treatment may bombard and roughen the surface of nanowires, thus producing new FE sites.

In contrast, for the case of $CF_4$ plasma treatment, the FE enhancement may be more related to the fluorinated carbon layer on the nanowires after $CF_4$ plasma treatment as was discussed in the XPS investigation. Previous study has shown that carbon coating on field emitters can enhance the field emission [33]. The dangling bonds will be produced in the fluorinated carbon materials under high electrical field [34], which can benefit the field emission [35]. Such a fluorinated layer also results in a decrease in the surface work function value. All these contribute to the enhanced field emission after 10 min of $CF_4$ plasma treatment, in addition to the larger emission density due to thinner and bent nanowires.

## 4. Conclusions

$O_2$ and $CF_4$ plasma from RIE system have been used to treat aligned CuO nanowire films to enhance their FE properties. Comparing the same nanowire before and after treatments shown that 10 min of plasma treatment reduces the tip diameter of nanowires by an average of 9 nm. Furthermore, the nanowires tips sharpened and/or bent which result in a larger effective field emission area. $O_2$ plasma removed the amorphous layer on the surface of as-grown nanowires and $CF_4$ plasma induced fluorinated carbon on the surface of nanowires and reduced the work function by about 0.5 eV. All these factors contributed to the improved FE current density and lowered the turn-on field. It is suggested that this plasma technique can also be extended to other nanomaterials, thus providing a direct means to control the tip diameters and to functionalize the surface morphologies of nanowires for various applications.

## Acknowledgments

The authors acknowledge the support from the National University of Singapore Academic Research Fund. T. Yu thanks the support from the Singapore Millennium Foundation.

## References

[1] A.A. Talin, K.A. Dean, J.E. Jaskie, Solid State Electron. 45 (2001) 963.
[2] N. de Jonge, J.-M. Bonard, Phil. Trans. Roy. Soc., Lond. Ser. A 362 (2004) 2239.
[3] J. Zhou, N.S. Xu, S.Z. Deng, J. Chen, J.C. She, Z.L. Wang, Adv. Mater. 15 (2003) 1835.
[4] J.J. Chiu, C.C. Kei, T.P. Perng, W.S. Wang, Adv. Mater. 15 (2003) 1361.

[5] C.J. Lee, T.J. Lee, S.C. Lyu, Y. Zhang, H. Ruh, H.J. Lee, Appl. Phys. Lett. 81 (2002) 3648.
[6] Z.S. Wu, S.Z. Deng, N.S. Xu, J. Chen, J. Zhou, J. Chen, Appl. Phys. Lett. 80 (2002) 3829.
[7] C.Y. Zhi, X.D. Bai, E.G. Wang, Appl. Phys. Lett. 81 (2002) 1690.
[8] K.S. Ahn, J.S. Kim, C.O. Kim, J.P. Hong, Carbon 41 (2003) 2481.
[9] S.C. Kung, K.C. Hwang, Appl. Phys. Lett. 80 (2002) 4819.
[10] S.H. Lai, K.P. Huang, Y.M. Pan, Y.L. Chen, L.H. Chan, P. Lin, H.C. Shih, Chem. Phys. Lett. 382 (2003) 567.
[11] J. Xu, J. Mei, X.H. Huang, X. Li, Z. Li, W. Li, K. Chen, Appl. Phys. A 80 (2004) 123.
[12] F.C.K. Au, K.W. Wong, Y.H. Tang, Y.F. Zhang, I. Bello, S.T. Lee, Appl. Phys. Lett. 75 (1999) 1700.
[13] T. Yu, X. Zhao, Z.X. Shen, Y.H. Wu, W.H. Su, J. Cryst. Growth 268 (2004) 590.
[14] X.C. Jiang, T. Herricks, Y.N. Xia, NanoLetters 2 (2002) 1333.
[15] C.T. Hsieh, J.M. Chen, H.H. Lin, H.C. Shih, Appl. Phys. Lett. 82 (2003) 3316.
[16] C.T. Hsieh, J.M. Chen, H.H. Lin, H.C. Shih, Appl. Phys. Lett. 83 (2003) 3383.
[17] Y.W. Zhu, T. Yu, F.C. Cheong, X.J. Xu, C.T. Lim, V.B.C. Tan, J.T.L. Thong, C.H. Sow, Nanotechnology 16 (2005) 88.
[18] Y.W. Zhu, F.C. Cheong, T. Yu, X.J. Xu, C.T. Lim, J.T.L. Thong, Z.X. Shen, C.K. Ong, Y.J. Liu, A.T.S. Wee, C.H. Sow, Carbon 43 (2005) 395.
[19] K.Y. Lim, C.H. Sow, J. Lin, F.C. Cheong, Z.X. Shen, J.T.L. Thong, K.C. Chin, A.T.S. Wee, Adv. Mater. 15 (2003) 300.
[20] C.D. Wagner, A.V. Naumkin, A.K. Vass, J.W. Allison, C.J. Powell, J.R. Rumble Jr, NIST X-ray Photoelectron Spectroscopy Database, Webversion:http://srdata.nist.gov/xps/.
[21] H.F. Goldstein, D.S. Kim, P.Y. Yu, L.C. Bourne, Phys. Rev. B 41 (1990) 7192.
[22] H. Hagemam, H. Bill, W. Sadowski, E. Walker, M. François, Solid State Commun. 73 (1990) 467.
[23] E.H. Lee, D.M. Hembree Jr, G.R. Rao, L.K. Mansur, Phys. Rev. B 48 (1993) 15540.
[24] Y. Park, V. Choong, Y. Gao, B.R. Hsieh, C.W. Tang, Appl. Phys. Lett. 68 (1996) 2699.
[25] F.P. Koffyberg, F.A. Benko, J. Appl. Phys. 53 (1982) 1173.
[26] H.H. Lin, C.Y. Wang, C.S. Han, J.M. Chen, C.T. Hsieh, J. Appl. Phys. 95 (2004) 5889.
[27] R.H. Fowler, L.W. Nordheim, Proc. Roy. Soc., Lond. Ser. A 119 (1928) 173.
[28] I.S. Altman, P.V. Pikhitsa, M. Choi, Appl. Phys. Lett. 84 (2004) 1126.
[29] D.A. Kirkpatrick, A. Mankofsky, K.T. Tsang, Appl. Phys. Lett. 60 (1992) 2065.
[30] R.C. Che, L.M. Peng, M.S. Wang, Appl. Phys. Lett. 85 (2004) 4753.
[31] Y.Z. Jin, W.K. Hsu, Y.L. Chueh, L.J. Chou, Y.Q. Zhu, K. Brigatti, H.W. Kroto, D.R.M. Walton, Angew. Chem., Int. Ed. 43 (2004) 5670.
[32] W. Hu, M. Matsumura, K. Furukawa, K. Torimitsu, J. Phys. Chem. B 108 (2004) 13116.
[33] J. Liu, V.V. Zhirnov, A.F. Myers, G.J. Wojak, W.B. Choi, J.J. Hren, S.D. Wolter, M.T. McClure, B.R. Stoner, J.T. Glass, J. Vac. Sci. Technol. B 13 (1995) 442.
[34] S.H. Lai, K.L. Chang, H.C. Shih, K.P. Huang, P. Lin, Appl. Phys. Lett. 85 (2004) 6248.
[35] S. Han, J. Ihm, Phys. Rev. B 61 (2000) 9986.